2021

Central Equatorial Pacific Cooling During the Last Glacial Maximum

Minda Moriah Monteagudo

Jean Lynch-Stieglitz

Thomas M. Marchitto

Matthew W. Schmidt
Old Dominion University, mwschmid@odu.edu

Original Publication Citation

Monteagudo, M. M., Lynch-Stieglitz, J., Marchitto, T. M., & Schmidt, M. W. (2021). Central equatorial Pacific cooling during the last glacial maximum. *Geophysical Research Letters, 48*(3), 1-10, Article e2020GL088592. https://doi.org/10.1029/2020GL088592

AGU ADVANCING EARTH AND SPACE SCIENCE

Geophysical Research Letters

RESEARCH LETTER
10.1029/2020GL088592

Central Equatorial Pacific Cooling During the Last Glacial Maximum

Minda Moriah Monteagudo[1], **Jean Lynch-Stieglitz**[1], **Thomas M. Marchitto**[2], and **Matthew W. Schmidt**[3]

[1]School of Earth and Atmospheric Sciences, Georgia Institute of Technology, Atlanta, GA, USA, [2]Department of Geological Sciences and Institute of Arctic and Alpine Research, University of Colorado, Boulder, CO, USA, [3]Department of Ocean, Earth and Atmospheric Sciences, Old Dominion University, Norfolk, VA, USA

Key Points:

- We present the first Mg/Ca data from the glacial Central Equatorial Pacific, which confirms cooling in agreement with model output
- A compilation of tropical Mg/Ca records indicates larger glacial cooling than previous proxy compilations
- Together these data suggest that Equilibrium Climate Sensitivity estimates based on earlier global proxy compilations may be underestimated

Supporting Information:

- Supporting Information S1
- Data Set S2

Correspondence to:
M. M. Monteagudo,
mmonteagudo3@gatech.edu

Citation:
Monteagudo, M. M., Lynch-Stieglitz, J., Marchitto, T. M., & Schmidt, M. W. (2021). Central equatorial Pacific cooling during the Last Glacial Maximum. *Geophysical Research Letters*, *48*, e2020GL088592. https://doi.org/10.1029/2020GL088592

Received 30 APR 2020
Accepted 31 DEC 2020

Abstract

Establishing tropical sea surface temperature (SST) during the Last Glacial Maximum (LGM) is important for constraining equilibrium climate sensitivity to radiative forcing. Until now, there has been little data from the central equatorial Pacific in global compilations, with foraminiferal assemblage-based estimates suggesting the region was within 1°C of modern temperatures during the LGM. This is in stark contrast to multi-proxy evidence from the eastern and western Pacific and model simulations which support larger cooling. Here we present the first estimates of glacial SST in the central equatorial Pacific from Mg/Ca in *Globigerinoides ruber*. Our results show that the central Pacific cooled by about 2.0°C during the LGM, in contrast with previous global compilations but in agreement with models. Our data support a larger magnitude of tropical LGM cooling, and thus a larger equilibrium climate sensitivity, than previous studies which relied on foraminiferal assemblages in the central tropical Pacific.

Plain Language Summary

Reconstructing how tropical Pacific climate changed during periods of variable atmospheric CO_2 levels may improve our understanding of how this region will respond to anthropogenic forcing. The Last Glacial Maximum, (LGM, 19–23,000 years before present), is the most recent time in earth history when atmospheric CO_2 was significantly different than pre-Industrial values. Proxy-based reconstructions of LGM sea surface temperatures (SSTs) are often used as a point of comparison with output from climate models. These models indicate ∼2°C cooling in the central equatorial Pacific during the LGM, in contrast with earlier microfossil-based estimates which suggest very little LGM cooling. Here, we use the chemistry of unicellular protists called foraminifera to estimate SSTs during the LGM in the central equatorial Pacific. Our data show that the central equatorial Pacific cooled by about 2°C during the LGM, in agreement with models and supporting the notion that this region may be more sensitive to CO_2 change than previously suggested.

1. Introduction

The tropical Pacific has been shown to be a dominant influence on global climate, from interannual to glacial-interglacial timescales; however, much uncertainty surrounds the evolution of the tropical Pacific Ocean-atmosphere system in response to varying atmospheric CO_2 levels. The Last Glacial Maximum (LGM, 19–23 ka) serves as an important interval for studying equilibrium climate sensitivity since the forcing is both large and fairly well-constrained, and multiple proxies exist to estimate the temperature response. LGM tropical sea surface temperature (SST), in particular, may be more significantly correlated with climate sensitivity than mean global temperature, given the lessened impact of high latitude forcings on tropical records (Hargreaves et al., 2012; Hopcroft & Valdes, 2015; Schmidt et al., 2014). Thus, the magnitude of tropical cooling during the LGM from proxy-based reconstructions is an important constraint on equilibrium climate sensitivity estimates (Hargreaves et al., 2012; Lea, 2004).

At present, both the magnitude and spatial pattern of tropical Pacific SST changes during the LGM remain uncertain. The Climate Long-Range Investigation Mapping and Prediction (CLIMAP) project's synthesis of glacial SST showed little to no SST change in the glacial central tropical Pacific, based largely on foraminiferal assemblages (CLIMAP Project Members, 1976). More recently, the Multiproxy Approach for the Reconstruction of the Glacial Ocean Surface (MARGO) project incorporated geochemical SST proxies, yet reiterated CLIMAP's finding of little to no SST change in the central tropical Pacific (Waelbroeck et al., 2009).

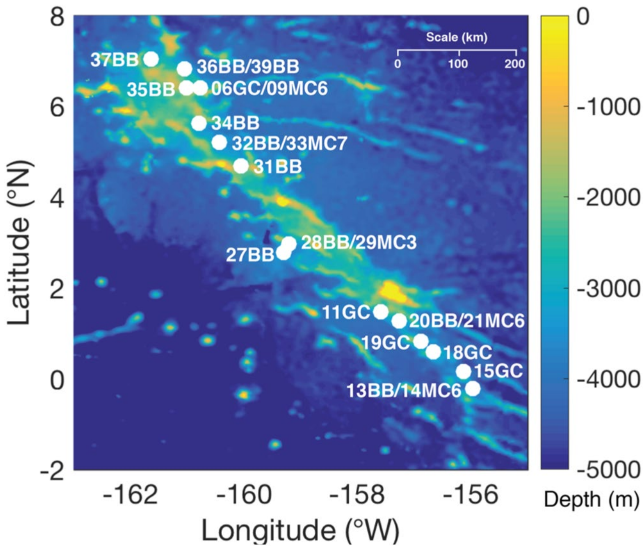

Figure 1. Bathymetric map (Amante & Eakins, 2009) of Line Islands core sites presented in this study (white markers).

However, it should be noted that there were very few geochemical measurements in the MARGO compilation from the central tropical Pacific and the MARGO project had to rely on foraminiferal assemblage data, much of it generated for the early CLIMAP study. In contrast, geochemical records from the eastern and western equatorial Pacific from Mg/Ca (Benway et al., 2006; Bolliet et al., 2011; Dang et al., 2020; de Garidel-Thoron et al., 2005, 2007; Hertzberg et al., 2016; Hollstein et al., 2018; Koutavas & Joanides, 2012; Koutavas et al., 2002; Lea et al., 2000, 2006; Leduc et al., 2007; Rosenthal et al., 2003; Sagawa et al., 2012; Steinke et al., 2006; Stott et al., 2002, 2007), alkenones (Kienast et al., 2001; Koutavas & Sachs, 2008; Leduc et al., 2007), TEX_{86} (Hertzberg et al., 2016), and clumped isotopes (Tripati et al., 2014) indicate 1°C–4°C cooling. Several proxy-based analyses indicate that the magnitude of overall tropical ocean cooling was likely 2.0°C–3.0°C (Ballantyne et al., 2005; Crowley, 2000), much larger than the moderate cooling suggested by CLIMAP and MARGO. Most recently, a multi-proxy data assimilation study showed 3.5°C of global tropical ocean cooling (Tierney et al., 2020). Terrestrial proxy records are also incompatible with CLIMAP/MARGO SSTs, as depressed tropical snowlines indicate ∼4°C–6°C cooling (Rind & Peteet, 1985; Webster & Streten, 1978). Given that lower atmospheric CO_2 should cause cooling, it remains difficult to explain why central tropical Pacific SSTs would be similar to modern during the LGM. Global climate model simulations driven with LGM boundary conditions suggests 2.0°C–2.5°C cooling in the central tropical Pacific and suggest a similar degree of cooling in the central tropical Pacific as in the eastern and western parts of the basin (Brady et al., 2013; DiNezio et al., 2011; Otto-Bliesner et al., 2009).

Here, we present the first estimates of central equatorial Pacific SSTs during the LGM using the Mg/Ca ratio of the surface-dwelling foraminifera *Globigerinoides ruber* from a meridional transect of sediment cores from the Line Islands. We also combine our data with existing tropical *G. ruber* Mg/Ca data to present a more complete view of tropical SST changes during the LGM.

2. Materials and Methods

2.1. Line Islands Sediment Cores and Age Models

The cores used in this study (Figure 1) were collected along the Line Islands Ridge, a NW-SE trending bathymetric rise in the central equatorial Pacific (Table 1), west of the Eastern Pacific Cold Tongue. Seasonal temperature and salinity variability at the Line Islands is low: 0.7°C–1.0°C and 0.2–0.5 PSU, respectively, increasing from the equator to 7°N (Schmidtko et al., 2013). Locations south of 2°N (∼27°C) are supplied with cooler water from the subsurface by equatorial upwelling, as well as from the Eastern Pacific via the South Equatorial Current. Warmer surface waters (∼28°C) north of 2° latitude are supplied from the Western Pacific via the North Equatorial Countercurrent.

The cores presented in this study span from 0.22°S to 7.04°N, 155.96 to 161.63°W, and 2,371–3,597 m water depth. Sedimentation rates range from ∼1.7 to 3.5 cm/kyr, decreasing with distance from the equator (Lynch-Stieglitz et al., 2015). Radiocarbon measurements were made on samples of the planktonic foraminifera *G. ruber* or *Trilobatus sacculifer* (350–500 μm size fraction) at the National Ocean Sciences Accelerator Mass Spectrometry facility at Woods Hole. Radiocarbon ages (Table S1) were converted to calendar ages using CALIB 7.1 and the Marine13 calibration curve, with the standard marine reservoir correction (R = 400 years) (Reimer et al., 2013). Age models for each core were constructed by linearly interpolating between radiocarbon measurements. Due to low-sedimentation rates above 2°N and recent carbonate dissolution, Late Holocene (0–4 ka) core-tops were available only for the southern portion of our transect. The age models were used to establish the

Table 1
Regional Estimates of Tropical (15°N–15°S) LGM Cooling (°C)

	Atlantic	Indian	Pacific	Global
MARGO	−2.9 ± 1.3	−1.4 ± 0.7	−1.2 ± 1.1	−1.7 ± 1.0
This study	−2.9 ± 0.4	−2.7 ± 0.1	−2.5 ± 0.1	−2.6 ± 0.1

depth ranges for Late Holocene (0–4 ka), Mid-Holocene (4–8 ka), and LGM (19–23 ka) time slices. Samples from depths within the above time slices were analyzed for Mg/Ca. Cores 27BB, 34BB and 36BB feature age reversals in the upper 8 cm; data above the age reversal are not used.

2.2. Analytical Methods for Line Islands Sediment Cores

G. ruber $\delta^{18}O$ data for all but one of the sediment core sites were published and discussed previously (Lynch-Stieglitz et al., 2015). We generated data for sediment core ML1208-32BB and the multicore tops as part of this study. $\delta^{18}O$ measurements were conducted on a Thermo MAT253 Stable Isotope Mass Spectrometer coupled to a Kiel IV Carbonate Device at Georgia Tech. 15 *G. ruber* individuals were analyzed from the 250–355 μm size fraction. $\delta^{18}O$ measurements were converted to PDB using an in-house standard and NBS-19. Reproducibility of the in-house standard was ±0.045‰ for $\delta^{18}O$ and ±0.014‰ for $\delta^{13}C$ (1 sigma).

For Mg/Ca measurements, ~60 individual *G. ruber* were selected from the 250–355 μm size fraction, gently crushed, homogenized, and split into two aliquots for replicate measurements, except where noted (Table S2). *G. ruber* is a symbiont-bearing foraminifera which confines its calcification depth to the upper ~50 (e.g., Schiebel & Hemleben, 2005) or 100 m (Rippert et al., 2016). *G. ruber* (sensu stricto) was picked whenever possible, though some sensu lato were necessary for sufficient sample masses. Oxygen isotopic measurements have shown no offset between morphotypes at the Line Islands, suggesting similar calcification depths (Lynch-Stieglitz et al., 2015). Mg/Ca samples were cleaned using both reductive and oxidative steps (Boyle & Rosenthal, 1996). The majority of measurements were done at University of Colorado, Boulder on a Thermo Element 2 ICP-MS. As indicated in the data supplement, some samples were cleaned and analyzed at Old Dominion University, with two cores (28BB and 37BB) cleaned and analyzed at Texas A&M University. Cleaning methods were consistent between labs and replicate measurements were used as inter-laboratory comparison (see supporting information Text S1; Figure S1) and show no systematic interlaboratory offset. Internal standards at CU Boulder are validated against powdered community standards BAM RS3, ECRM 752-1, and CMSI 1767 (Greaves et al., 2008). Al/Ca, Mn/Ca and Fe/Ca ratios were monitored for possible contamination and anomalously high values (>100 μmol/mol) were discarded (n = 1). Average reproducibility based on 94 replicate measurements was ±0.22 mmol/mol.

Mg/Ca measurements are converted to SST using the $\Delta[CO_3^{2-}]$-corrected calibration of Dekens et al. (2002), which gives the best match to climatology (see supporting information Text S2, Figure S2, Table S3). We used modern bottom water $[CO_3^{2-}]$ values computed using World Ocean Circulation Experiment (WOCE) P16 N measurements and CO2SysV2.1 for Excel. Sensitivity tests were performed using estimates of LGM Pacific $\Delta[CO_3^{2-}]$ changes, though these are generally believed to be small in magnitude (See supporting information Text S3, Figure S3). Late Holocene SSTs agree with climatological mean annual SSTs (Schmidtko et al., 2013) within the calibration error (Figure 2). It should be noted, however, that *G. ruber* Mg/Ca can also influenced by salinity (e.g., Lea et al., 1999; Nürnberg et al., 1996; Russell et al., 2004), carbonate chemistry conditions during calcification, expressed as either pH or $[CO_3^{2-}]$ (e.g., Evans et al., 2016; Gray et al., 2018). It has also recently been shown that the canonical ~9% sensitivity of Mg/Ca to temperature may overestimate the pure thermal component (Gray & Evans, 2019). Several multivariate calibrations have been published (Gray & Evans, 2019; Khider et al., 2015; Saenger & Evans, 2019; Tierney et al., 2019). The implications of these other Mg/Ca calibrations are discussed in the supporting information, but do not change the main conclusions of this work (supporting information Text S4, Figure S4).

2.3. Global *G. ruber* Mg/Ca Compilation

We compiled available LGM Mg/Ca data for *G. ruber* (white) from the literature (Table S5). We only compile data from *G. ruber*, as *T. sacculifer*, the other ubiquitous tropical surface-dwelling foraminifera species, has been shown to add significant amounts of gametogenic calcite at depth (Spero & Lea, 1993; Wycech

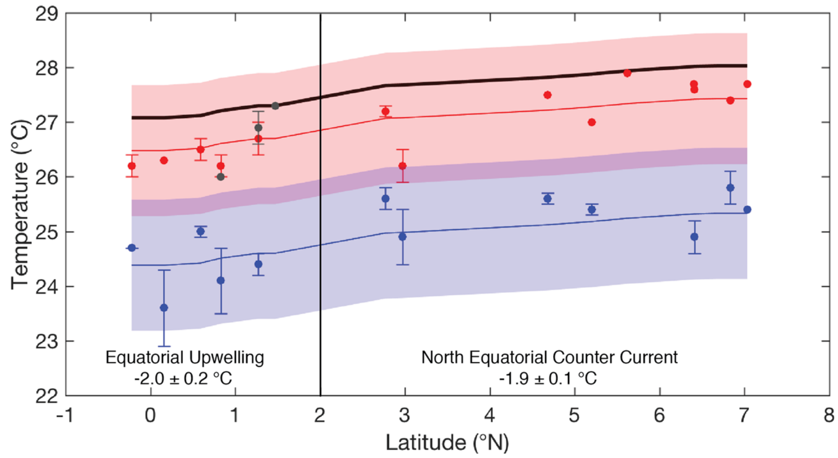

Figure 2. Mean *G. ruber* Mg/Ca-derived SST estimates for the Late Holocene (0–4 ka, gray symbols), Mid-Holocene (4–8 ka, red symbols), and LGM (19–23 ka, blue symbols) compared to modern mean annual SST (black line) (Schmidtko et al., 2013). All temperature estimates are calculated using the Dekens et al. (2002) calibration. Solid lines show the modern climatological SST (black), the modern SST shifted by −0.6°C (red) and −2.6°C (blue). The shaded regions denote the 1.2°C calibration standard error of estimate (Dekens et al., 2002). Error bars show the standard error of the mean for data within a given time slice. A cooling of 2.0 degrees between the Late Holocene and LGM is inferred. LGM, last glacial maximum; SST, sea surface temperature.

et al., 2018), which may complicate the interpretation of *T. sacculifer* Mg/Ca as a purely SST signal. Cores located between 15°N and 15°S with radiocarbon dated LGM sections and *G. ruber* (212–355 μm) Mg/Ca data were selected. *G. ruber* (sensu stricto) data were used where available and noted, however some studies did not distinguish which morphotype was used. *G. ruber* (pink) data from the Atlantic was not included except one study which used *G. ruber* pink occasionally to increase sample size (Lea et al., 2003). Mg/Ca values between 0 and 4 ka (Late Holocene) and 19–23 ka (LGM) were averaged, as determined by the age models in the original publications. Raw Mg/Ca values were first corrected to account for differing cleaning methods, with a 10% correction applied to cores that omit the reductive cleaning step, as it has been shown that the reductive step reduces Mg/Ca ratios by ~10% (Barker et al., 2003). Average Mg/Ca ratios were converted to SST using the Dekens et al. (2002) $\Delta[CO_3^{2-}]$ calibration using modern bottom water $[CO_3^{2-}]$ for all Late Holocene data and the LGM data in the Pacific Ocean. In the Atlantic, LGM $\Delta[CO_3^{2-}]$ values were adjusted by +19 μmol/kg above 2.8 km water depth and -21 μmol/kg below this depth (supporting information Text S5). The magnitude of LGM cooling is calculated by taking the difference between Late Holocene and LGM Mg/Ca SSTs. Where Late Holocene samples are not available, the magnitude of LGM cooling is reported relative to the modern climatology. Mg/Ca temperature estimates for the global compilation are adjusted by +0.6°C, the mean offset between modern climatological mean annual SST and the Late Holocene Mg/Ca SST found in the global data set (supporting information Text S5). This prevents the overestimation of the magnitude of LGM cooling for the core sites where cooling is reported relative to the modern climatological SST. The magnitude of cooling for locations with Late Holocene Mg/Ca are independent of the application of this offset.

3. Results and Discussion

3.1. LGM Temperature in the Central Equatorial Pacific

For the core sites that have Late Holocene aged sediments at the core top, Late Holocene Line Islands SSTs are 26.6°C–27.1°C, compared to climatological SSTs of 27.2°C–27.3°C (Figure 2). The Mid-Holocene (4–8 ka) is the most recent time interval for which data is available at all latitudes along our Line Islands Ridge transect. While there are only three locations for which Late Holocene data are available, there is no indication of significant changes in temperature between the Mid and Late Holocene (Figure 2). While all cores show moderately cooler temperature estimates for the Late and Mid-Holocene relative to the climatological data (Schmidtko et al., 2013), the offset (-0.6°C) is the same as was found between the Late Holocene and climatological SST in our global tropical data set. The lack of significant change between the Late and Mid Holocene is broadly consistent with PMIP2 and PMIP3 6 ka simulations that show only modest SST changes (0.2°C–0.4°C cooling) near the Line Islands (An & Choi, 2014).

Line Islands glacial Mg/Ca SST estimates range from 24.2°C to 26.4°C, indicating cooling at all core sites, between 1.4°C and 2.8°C (mean = 2.0°C) relative to the Late Holocene. Cores influenced by equatorial upwelling (−0.22 to 1.27°N) show 2.0°C ± 0.2°C (1 sigma standard error) of LGM cooling, as compared to more northerly cores influenced by the North Equatorial Counter Current which show 1.9°C ± 0.1°C. The glacial-interglacial difference in temperature is reported with the standard error, which approximates our ability to state the mean value in glacial-interglacial Mg/Ca temperature difference using our chosen calibration at this location. The error on the individual SST estimates can be approximated using the 1.2°C calibration error from Dekens et al. (2002). The true glacial-interglacial temperature difference in this region may differ due to systematic errors in the proxy and calibration which are difficult to quantify without the consideration of multiple proxies (e.g., Waelbroeck et al., 2009).

Our results do not agree with CLIMAP and MARGO, which suggest little to no SST change near the Line Islands and throughout most of the central Pacific. In contrast, our data are consistent with both model simulations that show ~2.0°C–2.5°C cooling near the Line Islands (Brady et al., 2013; DiNezio et al., 2011) as well as proxy records from the eastern and western equatorial Pacific (Benway et al., 2006; Bolliet et al., 2011; Dang et al., 2020; de Garidel-Thoron et al., 2007, 2005; Hertzberg et al., 2016; Hollstein et al., 2018; Koutavas & Joanides, 2012; Lea et al., 2000, 2006; Leduc et al., 2007; Rosenthal et al., 2003; Sagawa et al., 2012; Steinke et al., 2006; Stott et al., 2007, 2002; Xu et al., 2010). The recent LGM data assimilation study of Tierney et al. (2020) shows cooling at our core sites, but of a higher magnitude (−3.9°C) than we find in this study. Central tropical Pacific cooling is a robust feature of LGM model simulations, but has until now not been corroborated by proxy reconstructions in the region.

The Line Islands meridional SST gradient is sensitive to changes in zonal currents, local equatorial upwelling strength, and thermocline depth and tilt, all of which may reflect changes to Pacific Walker Circulation (DiNezio et al., 2011; Lynch-Stieglitz et al., 2015). Today, Northern Line Islands sites are 0.7°C ± 0.2°C warmer than Southern Line Islands sites. During the Mid-Holocene, the Line Islands meridional SST gradient remained similar (0.8°C ± 0.3°C). During the LGM, the meridional Line Islands SST gradient was increased to 1.1°C ± 0.4°C. While the meridional gradients are not distinguishable within the estimated errors, it is likely (72%) that the LGM temperature gradient was larger than modern (supporting information Text S6). An earlier study (Lynch-Stieglitz et al., 2015) based on this suite of sediment cores found an enhanced LGM gradient in the δ^{18}O of *G. ruber* calcite for these sediment cores, and discussed how the enhanced gradient relates to changes in tropical Pacific climate including the Walker Circulation. The Mg/Ca temperature data clarify that the increased gradient in foraminiferal δ^{18}O is partially due to the increased temperature gradient and partially to an increase in the δ^{18}O of seawater (supporting information Text S7, Figure S5, Table S4).

3.2. Tropical LGM Cooling From *G. ruber* Mg/Ca

Coupled ocean-atmosphere models consistently simulate stronger and more uniform LGM ocean cooling than MARGO in the tropical oceans (Braconnot et al., 2007; Brady et al., 2013; DiNezio et al., 2011; Otto-Bliesner et al., 2009). Our compilation of 76 LGM *G. ruber* Mg/Ca SST estimates also shows a larger tropical mean LGM cooling than MARGO, 2.6°C ± 0.1°C (1 sigma standard error on mean) as compared to 1.7°C ± 1.0°C (total error) (Figure 3, Tables 1 and S5). In the Atlantic, our compilation shows 2.9°C ± 0.4°C cooling, in agreement with 2.9°C ± 1.3°C from MARGO. However, in the Pacific and Indian oceans, our compilation indicates 2.5°C ± 0.1°C and 2.7°C ± 0.1°C cooling, respectively, larger than the 1.2°C ± 1.1°C and 1.4°C ± 0.7°C suggested by MARGO. With the addition of the new central Pacific data, our Mg/Ca compilation also shows more uniform cooling, without the large meridional gradients suggested by MARGO, but in good agreement with model results. It should be noted that our estimates, while systematically cooler than MARGO, do fall within their estimate of total error which accounts for proxy spread among a number of other factors. Our compilation is also broadly consistent with LGM alkenone compilations (e.g.,

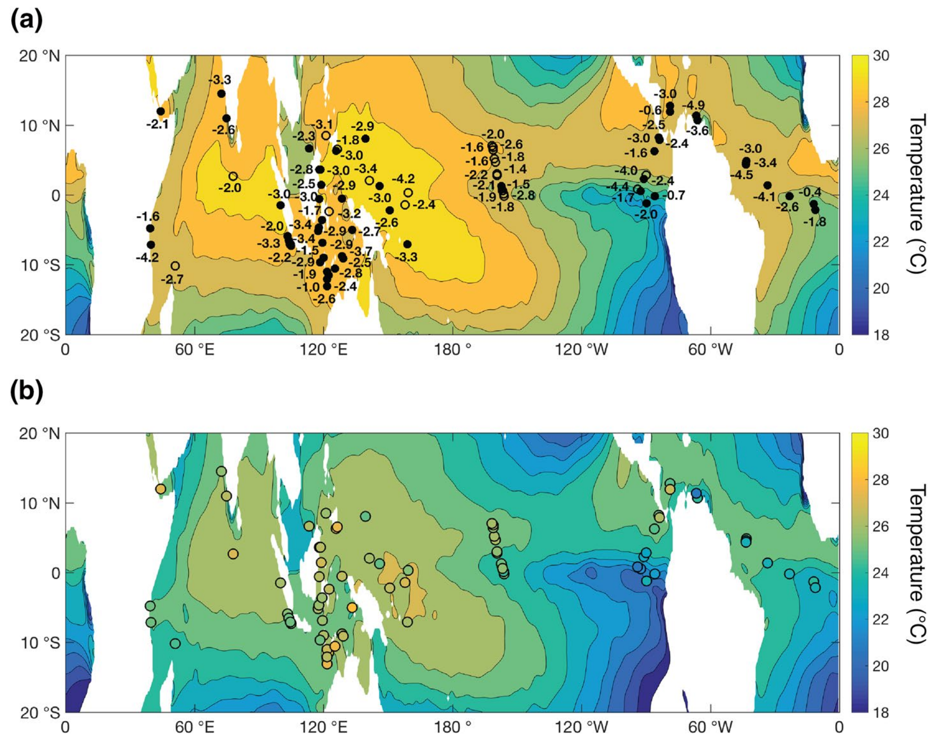

Figure 3. (a) Magnitude of mean LGM SST change (LGM-modern) from tropical (15°N to 15°S) *G. ruber* Mg/Ca studies (references in Table S5). Markers indicate core locations. Negative values indicate cooling relative to the Late Holocene (filled symbols), or modern climatological SSTs where Late Holocene data are not available (open symbols). Base map is mean annual SST (Schmidtko et al., 2013). (b) Base map is the same as (a), with the mean tropical LGM-modern cooling (−2.6°C) subtracted in order to better allow for the visual assessment of any systematic changes in the spatial gradients from the modern (base map) to the LGM (markers). Marker color denotes the absolute SST during the LGM based on *G. ruber* Mg/Ca. LGM, last glacial maximum; SST, sea surface temperature.

Rosell-Melé et al., 2004), although the magnitude of LGM cooling is sensitive to the choice of calibration (Tierney & Tingley, 2017) and may be affected by different seasonal influences than Mg/Ca (e.g., Timmermann et al., 2014). Our compilation gives a smaller LGM tropical cooling than a recent data assimilation study which shows 3.4°C of cooling in the 15°S–15°N latitude band (Tierney et al., 2020). However, the authors of this study note that the spatial average tropical SST change based on the geochemical proxy data alone is 0.9°C smaller than the change based on the data assimilation product, implying that the proxy data average change would be very similar to what we find in our compilation. They attribute this difference to enhanced cooling throughout the central and eastern tropical Pacific in their assimilated field, cooling which is not corroborated by the new central tropical Pacific Mg/Ca data presented here. The magnitude of glacial cooling estimated here based on *G. ruber* Mg/Ca is in line with model estimates (Brady et al., 2013; DiNezio et al., 2011; Otto-Bliesner et al., 2009), and provides support for the idea that CLIMAP data from the central Pacific may not be reliable, as has been previously suggested (Crowley, 2000; Mix et al., 1999).

It has been suggested that tropical Pacific SST change during the LGM (Lea, 2004) and overall tropical temperature change (Hargreaves et al., 2012) provide a constraint on equilibrium climate sensitivity. Studies using MARGO tropical SSTs (1.7°C ± 1.0°C mean LGM cooling) have estimated equilibrium climate sensitivity at 1.0°C–3.6°C (Waelbroeck et al., 2009) and 1.2°C–2.4°C (Annan & Hargreaves, 2013) (95% confidence intervals). Alternatively, a model-data analysis that assumed MARGO SST change was underestimated by 1°C found a climate sensitivity of 1.6°C–4.5°C (95% confidence interval), consistent with estimates from models run with LGM boundary conditions (e.g., Brady et al., 2013). Our compilation results, 2.6°C mean tropical cooling, would also suggest a similar climate sensitivity to what was estimated using 2.8°C cooling from a single Eastern Pacific Mg/Ca record (Lea 2004). The recent multi-proxy data assimilation study (Tierney et al., 2020) found climate sensitivity to be 2.4°C–4.5°C (95% confidence interval)—broadly consistent with the estimate from Schmidt et al. (2014) but with a higher lower bound.

4. Conclusions

We have produced the first planktonic foraminiferal Mg/Ca data for the glacial central equatorial Pacific, which show, on average ~2.0°C cooling, in line with model estimates but disagreeing with the CLIMAP and MARGO compilations. These data, together with existing Mg/Ca temperature estimates from the global tropics suggest a tropical cooling of ~2.6°C, implying that MARGO-based Equilibrium Climate Sensitivity estimates may be underestimated. Our new central Pacific data underscores the importance of continued work on both proxy development and the value of developing radiocarbon dated and geochemically based SST records from the open ocean. While the open ocean temperature estimates originating from the faunal counts of the CLIMAP program over 40 years ago were revolutionary for their time, these data alone are insufficient for constraining today's state-of-the-art climate models.

Data Availability Statement

All radiocarbon, Mg/Ca and oxygen isotope data presented in this study are included in the Supporting Information and are archived at the National Oceanic and Atmospheric Administration National Centers for Environmental Information database (https://www.ncdc.noaa.gov/paleo/study/29252).

Acknowledgments
The authors acknowledge the US National Science Foundation Grant OCE-1502927 to J. Lynch-Stieglitz. We also thank T.-Y. Chang for technical assistance.

References

Amante, C., & Eakins, B. W. (2009). *ETOPO1 1 arc-minute global relief model: Procedures, data sources and analysis*. NOAA Technical Memorandum NESDIS NGDC-24. National Geophysical Data Center. Retrieved from https://doi.org/10.1594/PANGAEA.769615

An, S. I., & Choi, J. (2014). Mid-Holocene tropical Pacific climate state, annual cycle, and ENSO in PMIP2 and PMIP3. *Climate Dynamics*, *43*(3–4), 957–970. https://doi.org/10.1007/s00382-013-1880-z

Annan, J. D., & Hargreaves, J. C. (2013). A new global reconstruction of temperature changes at the last glacial maximum. *Climate of the Past*, *9*(1), 367–376. https://doi.org/10.5194/cp-9-367-2013

Ballantyne, A. P., Lavine, M., Crowley, T. J., Liu, J., & Baker, P. B. (2005). Meta-analysis of tropical surface temperatures during the last glacial maximum. *Geophysical Research Letters*, *32*(5), 1–4. https://doi.org/10.1029/2004GL021217

Barker, S., Greaves, M., & Elderfield, H. (2003). A study of cleaning procedures used for foraminiferal Mg/Ca paleothermometry. *Geochemistry, Geophysics, Geosystems*, *4*(9), 1–20. https://doi.org/10.1029/2003GC000559

Benway, H. M., Mix, A. C., Haley, B. A., & Klinkhammer, G. P. (2006). Eastern Pacific Warm Pool paleosalinity and climate variability: 0-30 kyr. *Paleoceanography*, *21*, PA3008. https://doi.org/10.1029/2005PA001208

Bolliet, T., Holbourn, A., Kuhnt, W., Laj, C., Kissel, C., Beaufort, L., et al. (2011). Mindanao dome variability over the last 160 kyr: Episodic glacial cooling of the West Pacific Warm Pool. *Paleoceanography*, *26*(1), PA1208. https://doi.org/10.1029/2010PA001966

Boyle, E., & Rosenthal, Y. (1996). *Chemical hydrography of the South Atlantic during the Last Glacial Maximum: Cd vs. δ13C*. In The South Atlantic. Berlin, Heidelberg: Springer Berlin Heidelberg. Retrieved from https://doi.org/10.1007/978-3-642-80353-6_23

Braconnot, P., Otto-Bliesner, B., Harrison, S., Joussaume, S., Peterchmitt, J. Y., Abe-Ouchi, A., et al. (2007). Results of PMIP2 coupled simulations of the mid-holocene and last glacial maximum - Part 1: Experiments and large-scale features. *Climate of the Past*, *3*(2), 261–277. https://doi.org/10.5194/cp-3-261-2007

Brady, E. C., Otto-Bliesner, B. L., Kay, J. E., & Rosenbloom, N. (2013). Sensitivity to glacial forcing in the CCSM4. *Journal of Climate*, *26*(6), 1901–1925. https://doi.org/10.1175/JCLI-D-11-00416.1

CLIMAP Project Members (1976). Modeling the ice-age climate. *Science*, *191*(4232), 1138–1144. https://doi.org/10.1126/science.191.4232.1138

Crowley, T. J. (2000). CLIMAP SSTs re-revisited. *Climate Dynamics*, *16*, 241–255.

Dang, H., Jian, Z., Wang, Y., Mohtadi, M., Rosenthal, Y., Ye, L., et al. (2020). Pacific warm pool subsurface heat sequestration modulated Walker circulation and ENSO activity during the Holocene. *Science Advances*, *6*, 1–9.

de Garidel-Thoron, T., Rosenthal, Y., Bassinot, F., & Beaufort, L. (2005). Stable sea surface temperatures in the western Pacific warm pool over the past 1.75 million years. *Nature*, *433*, 294–298. https://doi.org/10.1038/nature03189

de Garidel-Thoron, T., Rosenthal, Y., Beaufort, L., Bard, E., Sonzogni, C., & Mix, A. C. (2007). A multiproxy assessment of the western equatorial Pacific hydrography during the last 30 kyr. *Paleoceanography*, *22*(3), 1–18. https://doi.org/10.1029/2006PA001269

Dekens, P. S., Lea, D. W., Pak, D. K., & Spero, H. J. (2002). Core top calibration of Mg/Ca in tropical foraminifera: Refining paleotemperature estimation. *Geochemistry, Geophysics, Geosystems*, *3*(4), 1–29. https://doi.org/10.1029/2001gc000200

DiNezio, P., Clement, A., Vecchi, G. A., Soden, B., Broccoli, A. J., Otto-Bliesner, B. L., & Braconnot, P. (2011). The response of the Walker circulation to last glacial maximum forcing: Implications for detection in proxies. *Paleoceanography*, *26*(3), 1–21. https://doi.org/10.1029/2010PA002083

Evans, D., Wade, B. S., Henehan, M., Erez, J., & Müller, W. (2016). Revisiting carbonate chemistry controls on planktic foraminifera Mg/Ca: Implications for sea surface temperature and hydrology shifts over the Paleocene–Eocene thermal maximum and Eocene–Oligocene transition. *Climate of the Past*, *12*(4), 819–835. https://doi.org/10.5194/cp-12-819-2016

Ferguson, J. E., Henderson, G. M., Kucera, M., & Rickaby, R. E. M. (2008). Systematic change of foraminiferal Mg/Ca ratios across a strong salinity gradient. *Earth and Planetary Science Letters*, *265*(1–2), 153–166. https://doi.org/10.1016/j.epsl.2007.10.011

Gray, W. R., & Evans, D. (2019). Nonthermal influences on Mg/Ca in planktonic foraminifera: A review of culture studies and application to the last glacial maximum. *Paleoceanography and Paleoclimatology*, *34*(3), 306–315. https://doi.org/10.1029/2018PA003517

Gray, W. R., Weldeab, S., Lea, D. W., Rosenthal, Y., Gruber, N., Donner, B., & Fischer, G. (2018). The effects of temperature, salinity, and the carbonate system on Mg/Ca in *Globigerinoides ruber* (white): A global sediment trap calibration. *Earth and Planetary Science Letters*, *482*, 607–620. https://doi.org/10.1016/j.epsl.2017.11.026

Greaves, M., Caillon, N., Rebaubier, H., Bartoli, G., Bohaty, S., Cacho, I., et al. (2008). Interlaboratory comparison study of calibration standards for foraminiferal Mg/Ca thermometry. *Geochemistry, Geophysics, Geosystems*, *9*(8), Q08010. https://doi.org/10.1029/2008GC001974

Hargreaves, J. C., Annan, J. D., Yoshimori, M., & Abe-Ouchi, A. (2012). Can the Last Glacial Maximum constrain climate sensitivity?. *Geophysical Research Letters*, *39*(24), L24702. https://doi.org/10.1029/2012GL053872

Hertzberg, J. E., Schmidt, M. W., Bianchi, T. S., Smith, R. K., Shields, M. R., & Marcantonio, F. (2016). Comparison of eastern tropical Pacific TEX86 and *Globigerinoides ruber* Mg/Ca derived sea surface temperatures: Insights from the Holocene and Last Glacial Maximum. *Earth and Planetary Science Letters*, *434*, 320–332. https://doi.org/10.1016/j.epsl.2015.11.050

Hollstein, M., Mohtadi, M., Rosenthal, Y., Prange, M., Tachikawa, K., Moffa, P., et al. (2018). Variations in Western Pacific Warm Pool surface and thermocline conditions over the past 110,000 years: Forcing mechanisms and implications for the glacial Walker circulation. *Quaternary Science Reviews*, *201*, 429–445. https://doi.org/10.1016/j.quascirev.2018.10.030

Hopcroft, P. O., & Valdes, P. J. (2015). Last glacial maximum constraints on the Earth System model HadGEM2-ES. *Climate Dynamics*, *45*(5–6), 1657–1672. https://doi.org/10.1007/s00382-014-2421-0

Khider, D., Huerta, G., Jackson, C., Stott, L. D., & Emile-Geay, J. (2015). A Bayesian, multivariate calibration for *Globigerinoides ruber* Mg/Ca. *Geochemistry, Geophysics, Geosystems*, *16*, 2916–2932. https://doi.org/10.1002/2015GC005844

Kienast, M., Steinke, S., Stattegger, K., & Calvert, S. E. (2001). Synchronous tropical south China sea SST change and Greenland warming during deglaciation. *Science*, *291*(5511), 2132–2134. https://doi.org/10.1126/SCIENCE.1057131

Koutavas, A., & Joanides, S. (2012). El Niño-southern oscillation extrema in the Holocene and last glacial maximum. *Paleoceanography*, *27*(4), 1–15. https://doi.org/10.1029/2012PA002378

Koutavas, A., Lynch-Stieglitz, J., Marchitto, T. M., & Sachs, J. P. (2002). El Niño-like pattern in ice age tropical Pacific sea surface temperature. *Science*, *297*, 226–230. http://doi.org/10.1126/science.1072376

Koutavas, A., & Sachs, J. P. (2008). Northern timing of deglaciation in the eastern equatorial Pacific from alkenone paleothermometry. *Paleoceanography*, *23*, PA4205. https://doi.org/10.1029/2008PA001593

Lea, David, W. (2004). The 100 000-yr cycle in tropical SST, greenhouse forcing, and climate sensitivity. *Journal of Climate*, *17*(11), 2170–2179. https://doi.org/10.1175/1520-0442(2004)017<2170:TYCITS>2.0.CO.2

Lea, D. W., Mashiotta, T. A., & Spero, H. J. (1999). Controls on magnesium and strontium uptake in planktonic foraminifera determined by live culturing. *Geochimica et Cosmochimica Acta*, *63*(16), 2369–2379. https://doi.org/10.1016/S0016-7037(99)00197-0

Lea, D. W., Pak, D. K., Belanger, C. L., Spero, H. J., Hall, M. A., & Shackleton, N. J. (2006). Paleoclimate history of Galápagos surface waters over the last 135,000 yr. *Quaternary Science Reviews*, *25*(11–12), 1152–1167. https://doi.org/10.1016/J.QUASCIREV.2005.11.010

Lea, D. W., Pak, D. K., Peterson, L. C., & Hughen, K. A. (2003). Synchroneity of tropical and high-latitude Atlantic temperatures over the last glacial termination. *Science*, *301*, 1361–1365.

Lea, D. W., Pak, D. K., & Spero, H. J. (2000). Climate impact of late quaternary equatorial Pacific sea surface temperature variations. *Science*, *289*(5485), 1719–1724. https://doi.org/10.1126/science.289.5485.1719

Leduc, G., Vidal, L., Tachikawa, K., Rostek, F., Sonzogni, C., Beaufort, L., & Bard, E. (2007). Moisture transport across Central America as a positive feedback on abrupt climatic changes. *Nature*, *445*(7130), 908–911. https://doi.org/10.1038/nature05578

Lynch-Stieglitz, J., Polissar, P. J., Jacobel, A. W., Hovan, S. A., Pockalny, R. A., Lyle, M., et al. (2015). Glacial-interglacial changes in central tropical Pacific surface seawater property gradients. *Paleoceanography*, *30*(5), 423–438. https://doi.org/10.1002/2014PA002746

Mehrbach, C., Culberson, C. H., Hawley, J. E., & Pytkowicx, R. M. (1973). Measurement of the apparent dissociation constants of carbonic acid in seawater at atmospheric pressure. *Limnology & Oceanography*, *18*(6), 897–907. https://doi.org/10.4319/lo.1973.18.6.0897

Mix, A. C., Morey, A. E., Pisias, N. G., & Hostetler, S. W. (1999). Foraminiferal faunal estimates of paleotemperature: Circumventing the no-analog problem yields cool ice age tropics. *Paleoceanography*, *14*(3), 350–359.

Nürnberg, D., Bijma, J., & Hemleben, C. (1996). Assessing the reliability of magnesium in foraminiferal calcite as a proxy for water mass temperatures. *Geochimica et Cosmochimica Acta*, *60*(5), 803–814. https://doi.org/10.1016/0016-7037(95)00446-7

Otto-Bliesner, B. L., Schneider, R., Brady, E. C., Kucera, M., Abe-Ouchi, A., Bard, E., et al. (2009). A comparison of PMIP2 model simulations and the MARGO proxy reconstruction for tropical sea surface temperatures at last glacial maximum. *Climate Dynamics*, *32*(6), 799–815. https://doi.org/10.1007/s00382-008-0509-0

Reimer, P. J., Bard, E., Beck, A., Blackwell, J. W., Ramsey, B., & Van Der Plicht, C. (2013). IntCal13 and Marine13 radiocarbon age calibration curves 0-50,000 years cal BP. *Radiocarbon*, *55*(4), 1869–1887. https://doi.org/10.2458/azu_js_rc.55.16947

Rind, D., & Peteet, D. (1985). Terrestrial conditions at the last glacial maximum and CLIMAP sea-surface temperature estimates: Are they consistent?. *Quaternary Research*, *24*(1), 1–22. https://doi.org/10.1016/0033-5894(85)90080-8

Rippert, N., Nürnberg, D., Raddatz, J., Maier, E., Hathorne, E., Bijma, J., & Tiedemann, R. (2016). Constraining foraminiferal calcification depths in the western Pacific warm pool. *Marine Micropaleontology*, *128*, 14–27. https://doi.org/10.1016/j.marmicro.2016.08.004

Rosell-Melé, A., Bard, E., Emeis, K. C., Grieger, B., Hewitt, C., Müller, P. J., & Schneider, R. R. (2004). Sea surface temperature anomalies in the oceans at the LGM estimated from the alkenone-U37K′ index: Comparison with GCMs. *Geophysical Research Letters*, *31*(3), 1–4. https://doi.org/10.1029/2003GL018151

Rosenthal, Y., Oppo, D. W., & Linsley, B. K. (2003). The amplitude and phasing of climate change during the last deglaciation in the Sulu Sea, western equatorial Pacific. *Geophysical Research Letters*, *30*(8), 1412. https://doi.org/10.1029/2002GL016612

Russell, A. D., Hönisch, B., Spero, H. J., & Lea, D. W. (2004). Effects of seawater carbonate ion concentration and temperature on shell U, Mg, and Sr in cultured planktonic foraminifera. *Geochimica et Cosmochimica Acta*, *68*(21), 4347–4361. https://doi.org/10.1016/j.gca.2004.03.013

Saenger, C. P., & Evans, M. N. (2019). Calibration and validation of environmental controls on planktic foraminifera Mg/Ca using global core-top data. *Paleoceanography and Paleoclimatology*, *34*(8), 1249–1270. https://doi.org/10.1029/2018pa003507

Sagawa, T., Yokoyama, Y., Ikehara, M., & Kuwae, M. (2012). Shoaling of the western equatorial Pacific thermocline during the last glacial maximum inferred from multispecies temperature reconstruction of planktonic foraminifera. *Palaeogeography, Palaeoclimatology, Palaeoecology*, *346–347*, 120–129. https://doi.org/10.1016/j.palaeo.2012.06.002

Schiebel, R., & Hemleben, C. (2005). Modern planktic foraminifera. *Paläontologische Zeitschrift*, *79*(1), 135–148. https://doi.org/10.1007/bf03021758

Schmidt, G. A., Annan, J. D., Bartlein, P. J., Cook, B. I., Guilyardi, E., Hargreaves, J. C., et al. (2014). Using palaeo-climate comparisons to constrain future projections in CMIP5. *Climate of the Past*, *10*(1), 221–250. https://doi.org/10.5194/cp-10-221-2014

Schmidtko, S., Johnson, G. C., & Lyman, J. M. (2013). MIMOC: A global monthly isopycnal upper-ocean climatology with mixed layers. *Journal of Geophysical Research: Oceans*, *118*(4), 1658–1672. https://doi.org/10.1002/jgrc.20122

Spero, H. J., & Lea, D. W. (1993). Intraspecific stable isotope variability in the planktic foraminifera *Globigerinoides sacculifer*: Results from laboratory experiments. *Marine Micropaleontology*, *22*(3), 221–234. https://doi.org/10.1016/0377-8398(93)90045-Y

Steinke, S., Chiu, H. Y., Yu, P. S., Shen, C. C., Erlenkeuser, H., Löwemark, L., & Chen, M. T. (2006). On the influence of sea level and monsoon climate on the southern South China Sea freshwater budget over the last 22,000 years. *Quaternary Science Reviews*, *25*(13–14), 1475–1488. https://doi.org/10.1016/j.quascirev.2005.12.008

Stott, L., Poulsen, C., Lund, S., & Thunell, R. (2002). Super ENSO and Global Climate Time Oscillations at Millennial Scales. *Science*, *297*(5579), 222–226. https://doi.org/10.1126/science.1071627

Stott, L., Timmermann, A., & Thunell, R. (2007). Southern Hemisphere and deep-sea warming led deglacial atmospheric CO_2 rise and tropical warming. *Science*, *318*(5849), 435–438. https://doi.org/10.1126/science.1143791

Tierney, J. E., Malevich, S. B., Gray, W., Vetter, L., & Thirumalai, K. (2019). Bayesian Calibration of the Mg/Ca Paleothermometer in Planktic Foraminifera. *Paleoceanography and Paleoclimatology*, *34*(12), 2005–2030. https://doi.org/10.1029/2019PA003744

Tierney, J. E., & Tingley, M. P. (2017). BAYSPLINE : A new calibration for the alkenone paleothermometer. *Paleoceanography and Paleoclimatology*, *33*, 281–301. https://doi.org/10.1002/2017PA003201

Tierney, J. E., Zhu, J., King, J., Malevich, S. B., Hakim, G. J., & Poulsen, C. J. (2020). Glacial cooling and climate sensitivity revisited. *Nature*, *584*, 569–573. https://doi.org/10.1038/s41586-020-2617-x

Timmermann, A., Sachs, J., & Timm, O. E. (2014). Assessing divergent SST behavior during the last 21 ka derived from alkenones and *G. ruber*-Mg/Ca in the equatorial Pacific. *Paleoceanography*, *29*(6), 680–696. https://doi.org/10.1002/2013PA002598

Tripati, A. K., Sahany, S., Pittman, D., Eagle, R. A., Neelin, J. D., Mitchell, J. L., & Beaufort, L. (2014). Modern and glacial tropical snowlines controlled by sea surface temperature and atmospheric mixing. *Nature Geoscience*, *7*(3), 205–209. https://doi.org/10.1038/ngeo2082

Waelbroeck, C., Paul, A., Kucera, M., Rosell-Melé, A., Weinelt, M., Schneider, R., et al. (2009). Constraints on the magnitude and patterns of ocean cooling at the last glacial maximum. *Nature Geoscience*, *2*(2), 127–132. https://doi.org/10.1038/ngeo411

Webster, P. J., & Streten, N. A. (1978). Late quaternary ice age climates of tropical Australasia: Interpretations and reconstructions. *Quaternary Research*, *10*(3), 279–309. https://doi.org/10.1016/0033-5894(78)90024-8

Wycech, J. B., Kelly, D. C., Kitajima, K., Kozdon, R., Orland, I. J., & Valley, J. W. (2018). Combined effects of gametogenic calcification and dissolution on δ18O measurements of the planktic foraminifer *Trilobatus sacculifer*. *Geochemistry, Geophysics, Geosystems*, *19*(11), 4487–4501. https://doi.org/10.1029/2018GC007908

Xu, J., Kuhnt, W., Holbourn, A., Regenberg, M., & Andersen, N. (2010). Indo-pacific warm pool variability during the Holocene and last glacial maximum. *Paleoceanography*, *25*(4), PA4230. https://doi.org/10.1029/2010PA001934

References From the Supporting Information

Adkins, J. F., & Schrag, D. P. (2001). Pore fluid constraints on deep ocean temperature and salinity during the last glacial maximum. *Geophysical Research Letters*, *28*(5), 771–774.

Anand, P., Elderfield, H., & Conte, M. H. (2003). Calibration of Mg/Ca thermometry in planktonic foraminifera from a sediment trap time series. *Paleoceanography*, *18*(2), 1050. https://doi.org/10.1029/2002PA000846

Anderson, D. M., & Archer, D. (2002). Glacial-interglacial stability of ocean pH inferred from foraminifer dissolution rates. *Nature*, *416*(6876), 70–73. https://doi.org/10.1038/416070a

Arbuszewski, J., deMenocal, P., Kaplan, A., & Farmer, E. C. (2010). On the fidelity of shell-derived δ18Oseawater estimates. *Earth and Planetary Science Letters*, *300*(3–4), 185–196. https://doi.org/10.1016/j.epsl.2010.10.035

Arrhenius, G. (1952). *Sediment cores from the east Pacific*. Reports of the Swedish Deep-Sea Expedition, 1947–1948 (Vol. 5, p. 201).

Bemis, B. E., Spero, H. J., & Lea, D. W. (1998). Reevaluation of the oxygen isotopic composition of planktonic foraminifera: Experimental results and revised paleotemperature equations. *Paleoceanography*, *13*(2), 150–160.

Boyer, T. P., Antonov, J. I., Baranova, O. K., Coleman, C., Garcia, H. E., Grodsky, A., et al. (2013). World Ocean database 2013, NOAA Atlas NESDIS 72. In S. L.evitus (Ed.) *Alexey Mishonoc. Technical Ed (pp. 209)*. NOAA Atlas. Retrieved From https://doi.org/10.7289/V5NZ85MT

Chalk, T. B., Foster, G. L., & Wilson, P. A. (2019). Dynamic storage of glacial CO_2 in the Atlantic Ocean revealed by boron 3 and pH records. *Earth and Planetary Science Letters*, *510*, 1–11. https://doi.org/10.1016/j.epsl.2018.12.022

Dai, Y., Yu, J., deMenocal, P., & Hyams-Kaphzan, O. (2019). Influences of temperature and secondary environmental parameters on planktonic foraminiferal Mg/Ca: A new core-top calibration. *Geochemistry, Geophysics, Geosystems*, *20*, 4370–4381. https://doi.org/10.1029/2019gc008526

Dickson, A. G. (1990). Standard potential of the reaction: AgCl(s) + 1 2H2(g) = Ag(s) + HCl(aq), and and the standard acidity constant of the ion HSO4- in synthetic sea water from 273.15 to 318.15 K. *The Journal of Chemical Thermodynamics*, *22*(2), 113–127. https://doi.org/10.1016/0021-9614(90)90074-Z

Dickson, A. G., & Millero, F. J. (1987). A comparison of the equilibrium constants for the dissociation of carbonic acid in seawater media. *Deep Sea Research Part A, Oceanographic Research Papers*, *34*(10), 1733–1743. https://doi.org/10.1016/0198-0149(87)90021-5

Farrell, J. W., & Prell, W. L. (1989). Climatic change and CaCO3 preservation: An 800,000 years bathymetric Reconstruction from the central equatorial Pacific Ocean. *Paleoceanography*, *4*(4), 447–466. https://doi.org/10.1029/PA004i004p00447

Fehrenbacher, J., & Martin, P. (2011). Western equatorial Pacific deep water carbonate chemistry during the last glacial maximum and deglaciation: Using planktic foraminiferal Mg/Ca to reconstruct sea surface temperature and seafloor dissolution. *Paleoceanography*, *26*(2), PA2225. https://doi.org/10.1029/2010PA002035

Hertzberg, J. E., & Schmidt, M. W. (2013). Refining *Globigerinoides ruber* Mg/Ca paleothermometry in the Atlantic Ocean. *Earth and Planetary Science Letters*, *383*, 123–133. https://doi.org/10.1016/j.epsl.2013.09.044

Kim, S. T., & O'Neil, J. R. (1997). Equilibrium and nonequilibrium oxygen isotope effects in synthetic carbonates. *Geochimica et Cosmochimica Acta*, *61*(16), 3461–3475. https://doi.org/10.1016/S0016-7037(97)00169-5

Kisakürek, B., Eisenhauer, A., Böhm, F., Garbe-Schönberg, D., & Erez, J. (2008). Controls on shell Mg/Ca and Sr/Ca in cultured planktonic foraminiferan, *Globigerinoides ruber* (white). *Earth and Planetary Science Letters*, *273*(3–4), 260–269. https://doi.org/10.1016/j.epsl.2008.06.026

Lalicata, J. J., & Lea, D. W. (2011). Pleistocene carbonate dissolution fluctuations in the eastern equatorial Pacific on glacial timescales: Evidence from ODP Hole 1241. *Marine Micropaleontology*, *79*(1–2), 41–51. https://doi.org/10.1016/J.MARMICRO.2011.01.002

LeGrande, A. N., & Schmidt, G. A. (2006). Global gridded data set of the oxygen isotopic composition in seawater. *Geophysical Research Letters*, *33*(12), 1–5. https://doi.org/10.1029/2006GL026011

Levitus, S., & Boyer, T. P. (1994). *World Ocean Atlas 1994*. Temperature (Vol. 4). NOAA Atlas NESDIS.

Marchitto, T. M., Lynch-Stieglitz, J., & Hemming, S. R. (2005). Deep Pacific $CaCO_3$ compensation and glacial-interglacial atmospheric CO_2. *Earth and Planetary Science Letters*, *231*, 317–336. https://doi.org/10.1016/j.epsl.2004.12.024

Mathien-Blard, E., & Bassinot, F. (2009). Salinity bias on the foraminifera Mg/Ca thermometry: Correction procedure and implications for past ocean hydrographic reconstructions. *Geochemistry, Geophysics, Geosystems*, *10*(12), Q12011. https://doi.org/10.1029/2008GC002353

Pierrot, D., Lewis, E., & Wallace, D. W. R. (2006). *MS Excel Program Developed for CO2 System Calculations*. ORNL/CDIAC-105a. https://doi.org/10.3334/cdiac/otg.co2sys_xls_cdiac105a

Qin, B., Li, T., Xiong, Z., Algeo, T. J., & Chang, F. (2017). Deepwater carbonate ion concentrations in the western tropical Pacific since 250 ka: Evidence for oceanic carbon storage and global climate influence. *Paleoceanography*, *32*(4), 351–370. https://doi.org/10.1002/2016PA003039

Regenberg, M., Regenberg, A., Garbe-Schönberg, D., & Lea, D. W. (2014). Global dissolution effects on planktonic foraminiferal Mg/Ca ratios controlled by the calcite-saturation state of bottom waters. *Paleoceanography*, *29*, 127–142. https://doi.org/10.1002/2013PA002492

Rongstad, B. L., Marchitto, T. M., & Herguera, J. C. (2017). Understanding the effects of dissolution on the Mg/Ca Paleothermometer in Planktic foraminifera: Evidence from a novel individual foraminifera method. *Paleoceanography*, *32*(12), 1386–1402. https://doi.org/10.1002/2017PA003179

Yu, J., Broecker, W. S. W. S., Elderfield, H. H., Zhangdong, J., McManus, J. F., Zhang, F., et al. (2010). Loss of carbon from the deep sea since the last glacial maximum. *Science*, *330*(6007), 1084–1087. https://doi.org/10.1126/science.1193221